Errors of attention adaptively warp spatial memory

James A. Brissenden[1], Yitong Yin[1], Michael Vesia[2], and Taraz G. Lee[1]

[1] Department of Psychology, University of Michigan, Ann Arbor, MI, United States

[2] School of Kinesiology, University of Michigan, Ann Arbor, MI, United States

Abstract

Adaptation is the process by which we adjust internal models of the body, world, and mind in response to sensory feedback. While adaptation is studied extensively in the context of motor control, there is limited evidence that cognitive functions such as working memory are subject to the same error-driven adaptive control mechanism. To examine the possibility that working memory representations undergo adaptation, we had participants perform a task that interleaved a perceptual discrimination task and a spatial working memory task. Perceptual discrimination trials (85% of trials) presented an initial peripheral cue to exogenously capture attention, immediately followed by a displaced target stimulus. This sequence of events served to repeatedly induce a covert attentional allocation error. Interleaved spatial working memory trials (15% of trials) presented a stimulus at a pseudorandom peripheral location followed by a delay interval. On half of the working memory trials, the stimulus was surreptitiously presented at the same location as the initial attentional cue. We found that as attentional errors accumulated over the course of the experiment, participants' working memory recall shifted in the direction of the attentional error. The magnitude of this shift was proportional to the number of induced errors. Recall performance rapidly recovered following the offset of error trials. Multiple control experiments ruled out alternative explanations for these results such as oculomotor confounds and attentional biases unrelated to error. These findings indicate that the computational mechanisms governing the adaptive control of motor commands appear to similarly serve to adjust and calibrate memory processes.

Introduction

Effectively interacting with the world around us requires continuous adjustment of behavior. Consider the act of driving a different car than the one you are used to driving. You might find that the sensitivity of the brake pedal is different, the acceleration response is quicker or slower, or the steering feels lighter or heavier. Initially, you will make numerous errors, such as braking harder than necessary. After driving the new car for some time, you adapt to these differences and your control of the vehicle becomes smooth and accurate. Adaptation is the process by which we fine-tune behavior in response to internal disturbances such as fatigue, injury, and disease and external perturbations such as the weight of an object we lift up or the terrain over which we are moving.[1] The adaptation of motor actions such as saccades has been studied extensively in both humans and non-human primates[2–7] and has been shown to be distinct from other types of learning (e.g. reinforcement learning or explicit strategy-based learning).[8–12] Typical saccade adaptation tasks involve displacing a peripheral target mid-saccade to induce a mismatch between where the eye lands and the position of the target.[2] This mismatch represents an error between the predicted outcome of the action command and the actual outcome. Over repeated trials (and repeated error signals), eye movement commands are adapted such that saccades land closer to the shifted target location.

While adaptation is typically studied in the context of motor control, there is reason to suspect that higher-level cognitive functions such as working memory may obey similar adaptive control mechanisms. For example, when driving an unfamiliar car, you may also find that critical visual inputs that must be attended or remembered such as the speedometer or rearview mirror are in a different location than expected. Effective performance would necessitate a change in how cognitive resources are allocated within this new environment. However, there is scant experimental evidence that working memory and other cognitive functions are subject to the same mechanisms of adaptive control as (eye) movements.

Here, we aimed to investigate whether visuospatial working memory storage is subject to adaptive control. A challenge in studying the role of adaptive control in working memory storage is how to elicit a working memory prediction error. Attention has been characterized as a gatekeeper that serves to determine which visual inputs are given priority for storage in working memory.[13–19] This relationship raises the possibility that the misallocation of attention could serve as an error signal for the adaptive control of working memory. We created a paradigm that interleaves an independent visual working memory task among trials that induce errors in the covert allocation of spatial attention. We aimed to determine whether working memory undergoes adaptation in response to spatial errors. If so, we should observe

a change in the working memory representation of the specific location associated with spatial attention allocation errors. Such as result would indicate that the phenomenon of adaptation is a domain-general learning process and would have far-ranging implications for our understanding of learning mechanisms underlying both motor and cognitive control.

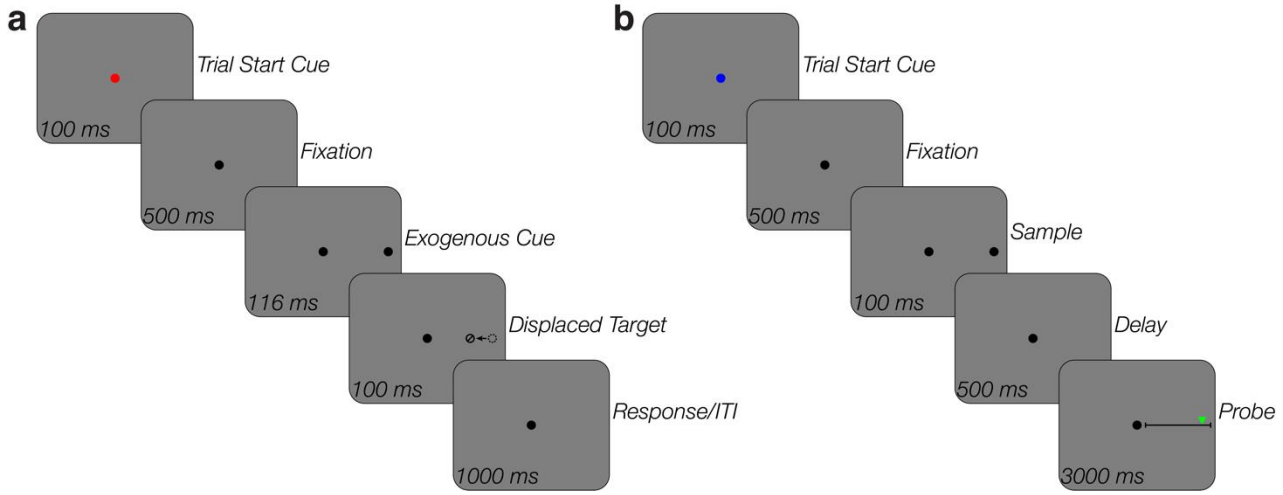

Figure 1. Exogenous attention error and spatial working memory experimental paradigm. a, Example trial sequence for the perceptual discrimination task that induces attentional errors. At the start of each trial, the central fixation dot briefly turns red to indicate the start of the trial and to reorient participants to the center of the display. Following a blank fixation interval, a small disc stimulus is presented in the periphery. Immediately following the offset of this initial cue, a small circular stimulus containing an oriented line is presented at a displaced location from the initial cue. Participants are instructed to indicate with a key-press whether the line was oriented at 45° or 135°. **b**, Spatial working memory trial sequence. A fixation dot turns blue to indicate the start of a working memory trial. A disc stimulus is then presented along the horizontal meridian within one hemifield. 50% of trials present the stimulus at a random location, while the other 50% of trials present the stimulus at the same location as the initial attention cue. Following a delay period, participants are probed to recall the location of the sample stimulus. Participants adjust a slider stimulus to match the location of the remembered item.

Results

Across 5 independent experiments, we had participants perform a task that interleaved a perceptual discrimination task with irrelevant spatial cues to exogenously capture attention (Fig. 1a) with a spatial working memory task (Fig. 1b). The perceptual discrimination task reflexively drew attention to a peripheral location before presenting a target to be discriminated at a location shifted relative to the initial cue location. As a result, a covert attentional allocation error was induced on each trial (Att-error trials; ~85% of trials). An independent working memory task was interleaved among these Att-error trials (~15% of trials). 50% of working memory trials presented the to-be-remembered stimulus at a random location along the horizontal meridian within one hemifield (WM-random trials) and the other half presented the stimulus at the same location as the initial attention cue (i.e. the location associated with the induced attentional error) (WM-fixed trials). We aimed to determine whether working memory exhibits signatures of adaptive control which would be evidenced by a shift in working memory recall in the direction of the induced error.

Covert attentional errors induce shift in spatial memory recall

Our first experiment consisted of 5 blocks of trials each comprising a mix of covert attentional error trials (220 Att-error trials) and working memory trials (20 WM-random trials and 20 WM-fixed). We observed overwhelming evidence for a shift in spatial recall across WM-fixed trials (Mean difference between block 1 and block 5: –15.19% ± 3.52% of backstep error; Bayes Factor (BF) = 3.35×10^{25}; Fig. 2a). 70% of participants (28/40) exhibited some degree of adaptation (>5% shift in the direction of the covert attentional error). To characterize the timecourse of learning, we averaged memory recall across participants for each WM-fixed trial and then fit 3 models (Linear, Single Exponential, and Double Exponential) and performed model comparison. The timecourse was best fit by an exponential decay model consistent with prior motor adaptation studies whereby accumulating attentional errors lead to a gradual shift in internal memory representations in the direction of the induced error (Linear ELPD = 340.4; Single Exponential ELPD = 353.7; Double Exponential ELPD = 353.0). There was a negligible difference in fit between the two exponential decay models. Exponential decay was apparent in individual subjects (see Supplementary Fig. 1).

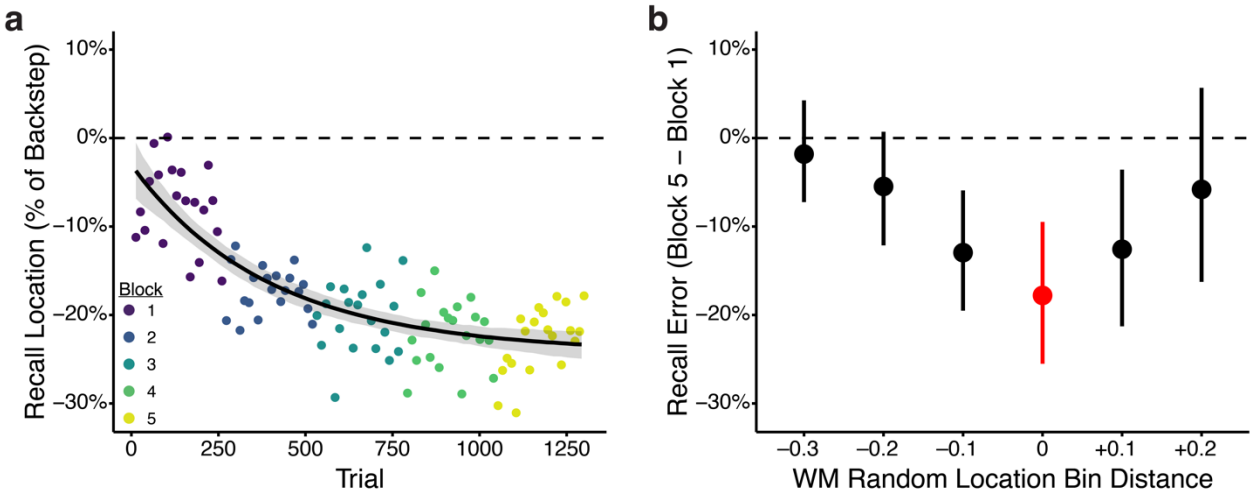

Figure 2. Timecourse and spatial specificity of working memory adaptation in response to spatial attention errors. a, Timecourse of working memory recall. Individual data points represent mean recall location (N=40) as a percentage of the backstep size on Att-error trials across subjects for each WM-fixed trial. The target stimulus appeared at the same location in all depicted data points (i.e. 0%). The *x*-axis represents the absolute trial number across all trial types (Att-error, WM-random, and WM-fixed). Each WM-fixed trial was preceded by 11 Att-error trials (and 1 WM-random trial). Color denotes block number. The timecourse of working memory adaptation follows an exponential decay function. The black line represents the mean of the model posterior predictive distribution as a function of trial number and the shaded area denotes the 95% credible interval of the expected values. **b,** Transfer of working memory adaptation across space. The *y*-axis shows percent change in spatial recall from the first to last block as a function of distance from the location associated with the covert attentional error. WM-random trials were binned according to distance from the adapted location. Red denotes the bin containing the adapted location. The *x*-axis represents center-to-center distance between bins in normalized 'height' units, which scale stimuli relative to the height of each participant's screen (see methods). Error bars represent bootstrap standard error.

How spatially specific is this adaptation? Prior saccade adaptation studies have demonstrated limited transfer of gain adaptation to locations nearby in space which indicates the existence of a so-called "adaptation field".[4,5,20] We grouped WM-random trials based on distance from the adapted location and found that adaptation was maximal at the adapted

location. Adaptation magnitude decreased with increasing distance from the spatial location associated with the covert attentional error (BF = 41.77; Linear Slope = 5.65% per bin, 95% Credible Interval (CI) [2.43%, 8.99%]; Fig. 2b).

Working memory adaptation cannot be explained by foveal bias

Although experiment 1 established a gradual shift in spatial memory representations that increased in magnitude along with the accumulation of induced attentional errors, it is possible that this finding could be due to factors aside from adaptation. The prior experiment could not rule out the possibility that participants are simply biased to report the remembered stimulus closer to the central portion of the visual field with repeated working memory trials. Experiment 1 also could not determine whether the observed adaptive shift in working memory recall is followed by rapid de-adaptation, a hallmark feature of motor adaptation in which full or partial unlearning of an adaptation is faster than the initial learning.[21] In Experiment 2, the first and last block consisted entirely of working memory trials (75 WM-random trials and 25 WM-fixed trials). This enabled us to determine if there were any sequential biases in spatial recall, as well as establish an estimate of a pre-adaptation baseline. There was limited evidence for a change in spatial recall across trials during the first pre-adaptation block (BF = 0.18; Linear Slope = –0.04% of backstep per trial, 95% CI [–0.09%, 0.02%]), indicating that performing repeated working memory trials (in the absence of induced covert attentional error) does not induce a foveal bias in spatial memory representations. We again found robust evidence for adaptation of working memory recall between the pre-adaptation block and the final adaptation block (-20.28% ± 3.50%; BF = 1.71×10^{47}; Supplementary Fig. 3a). We additionally found strong evidence for de-adaptation between the last adaptation block and the post-adaptation block (10.86% ± 1.84%; BF = 1.89×10^{18}), indicating that working memory rapidly de-adapts following the offset of attentional errors. De-adaptation magnitude was strongly correlated with the magnitude of adaptation across subjects ($r(38) = –0.64$, BF = 1975.41). Model comparison indicated that an exponential decay model best fit the timecourse of adaptation across adaptation blocks (Linear ELPD: 260; Single Exponential ELPD = 289.3; Double Exponential ELPD = 291.5; Fig. 3a; Also see Supplementary Figure 2 for individual subject data and fits), with negligible difference between the two exponential decay models. We replicated the finding from Experiment 1 that adaptation was maximal on WM-random trials at the adapted location and adaptation transfer decreased with distance (BF = 95,583; Linear Slope = 6.61% per bin, 95% CI [4.30%, 9.18%]; Fig. 3b).

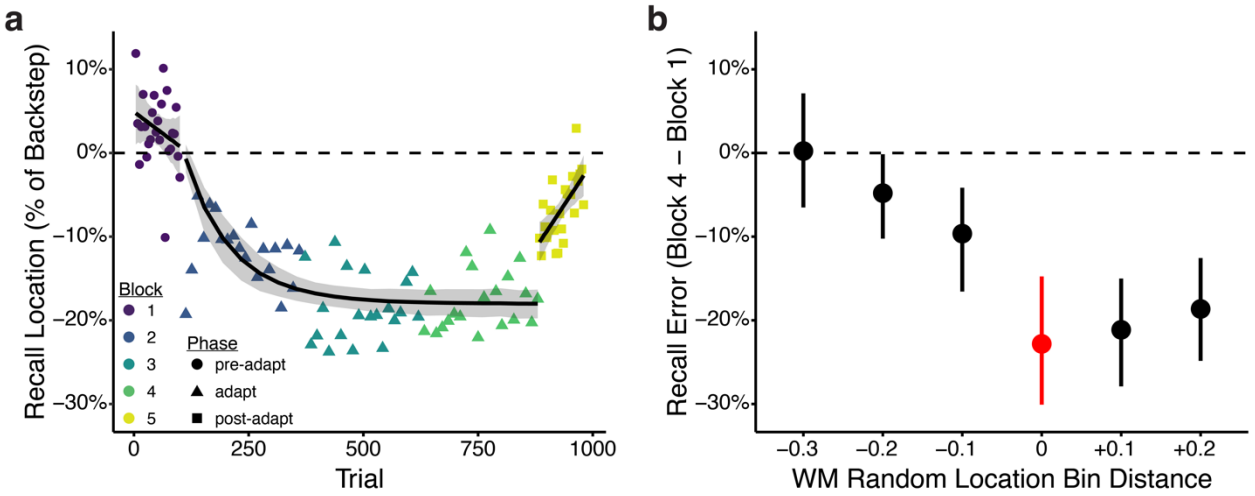

Figure 3. Working memory adaptation displays hallmark features of visuomotor adaptation. a, Timecourse of spatial recall on WM-fixed trials. Individual data points represent mean recall location (N=40) as a percentage of the backstep size on Att-error trials across subjects for each WM-fixed trial. Color denotes block number (1-5) and shape represents the phase of the experiment (pre-adapt, adapt, or post-adapt). The pre-adapt and post-adapt phases consisted solely of working memory trials (75 WM-random trials and 25 WM-fixed trials in each block) to assess baseline performance and rate of de-adaptation, respectively. The black lines spanning the pre- and post-adapt phases represent the mean of a linear model posterior predictive distribution, while the black line spanning the adapt phase is the mean of an exponential decay model posterior predictive distribution. The shaded area denotes the 95% credible interval of the expected value distribution for each model. **b**, Transfer of working memory adaptation across space. The *y*-axis shows percent change in spatial recall from the pre-adapt block to last block of the adaptation period as a function of distance from the location associated with the covert attentional error. WM-random trials were binned according to distance from the adapted location. Red denotes the bin containing the adapted location. The *x*-axis represents center-to-center distance between bins in normalized 'height' units, which scale stimuli relative to the height of the participant's screen (see methods). Error bars represent bootstrap standard error.

Working memory adaptation is driven by error

Canonical examples of motor adaptation are associated with sensory prediction errors. If the observed shift in spatial working memory recall can be explained by similar learning mechanisms to motor adaptation then this shift should be associated with error. To determine whether the adaptive shift in working memory recall is error-driven, we eliminated the error from attention trials by presenting the initial exogenous cue and target stimulus at the same location. This location was still shifted inward relative to the location of the mnemonic stimulus presented on WM-fixed trials. As a result, the behaviorally relevant location was displaced relative to the working memory stimulus but no error was induced over the course of the experiment. If we observe the same shift in working memory representations it would suggest that the observed shift in memory recall is not driven by covert attentional errors but is rather a bias towards a behaviorally relevant location. All other aspects of the experiment other than the lack of error on attention trials were identical to Experiment 2. We found evidence in favor of no difference in WM-fixed recall between the 1st block consisting entirely of working memory trials and the last intermixed attention and working memory block (-2.04% ± 1.86%; BF = 0.42; Supplementary Fig. 3b), indicating that repeatedly attending a nearby location does not bias working memory representations towards that location.

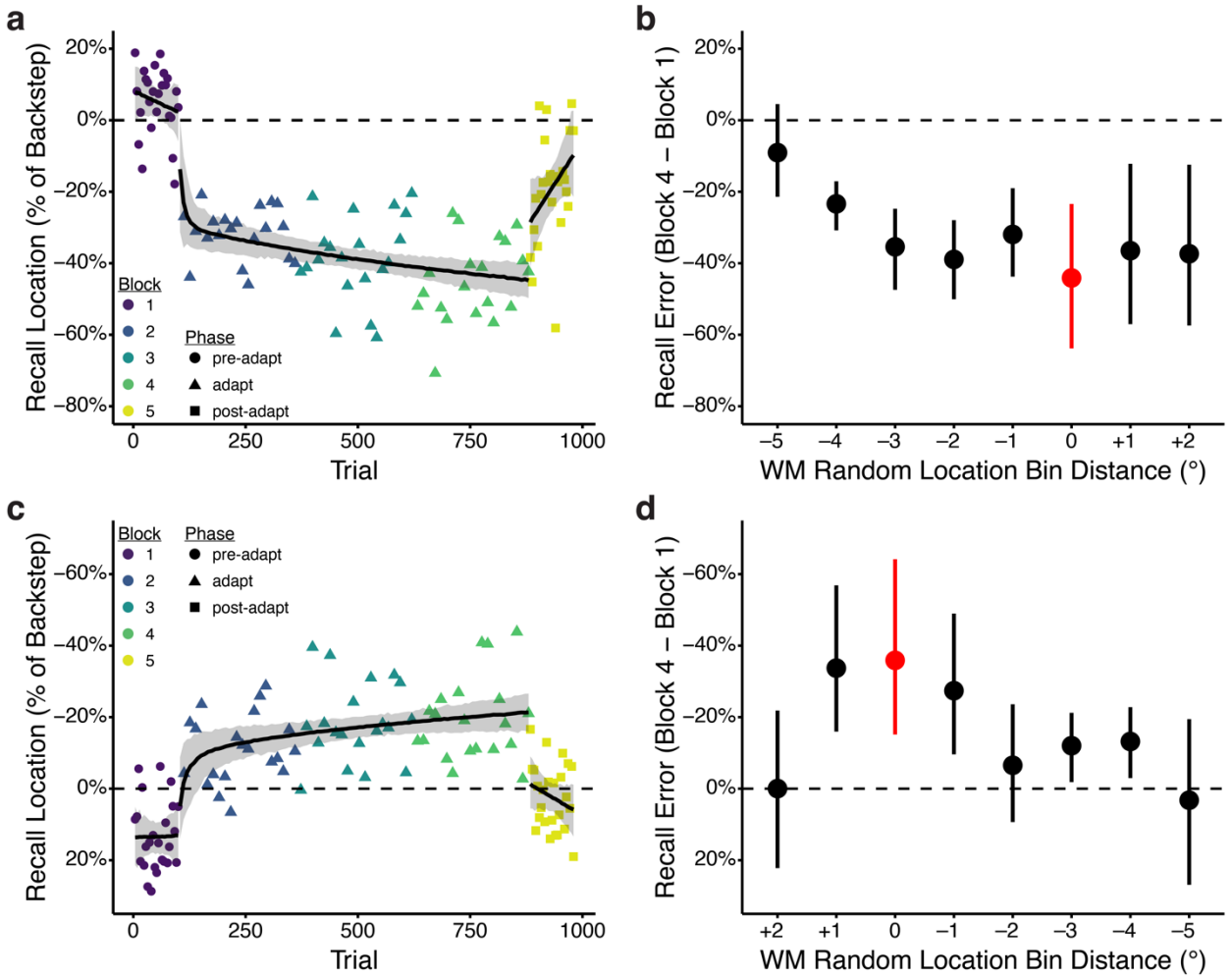

Figure 4. Replication of working memory adaptation across the visual field and controlling for potential oculomotor confounds. a, c, Timecourses of spatial recall on WM-fixed trials for Experiments 4 and 5. Experiments 4 and 5 were conducted in-person with concurrent eye-tracking to control for potential oculomotor confounds. Experiment 4 presented stimuli in the right hemifield and Experiment 5 presented stimuli in the left hemifield. Individual data points represent mean recall location (experiment 4: N=11; experiment 5: N=11) as a percentage of the backstep size (3°) on Att-error trials across subjects for each WM-fixed trial. Color denotes block number (1-5) and shape represents the phase of the experiment (pre-adapt, adapt, or post-adapt). The black lines spanning the pre- and post-adapt phases represent the mean of a linear model posterior predictive distribution, while the black line spanning the adapt phase is the mean of an exponential decay model posterior predictive distribution. The shaded area denotes the 95% credible interval of the expected value distribution for each model. **b, d,** Transfer of working memory adaptation across space. The *y*-axis shows percent change in spatial recall from the pre-adapt block to last block of the adaptation period as a function of distance from the location associated with the covert attentional error. WM-random trials were binned according to distance from the adapted location. Red denotes the bin containing the adapted location. The *x*-axis represents center-to-center distance between bins in degrees of visual angle. Error bars represent bootstrap standard error.

Working memory adaptation cannot be explained by eye movements

As Experiments 1-3 were conducted with online samples rather than in our laboratory, these experiments could not conclusively rule out a motor explanation of the apparent adaptation of working memory representations. It is possible that participants were making saccadic eye movements to the presented stimuli despite our repeated instructions to maintain fixation. In this scenario, saccades would be adapted by the perceived mismatch between the saccade landing point and the presented grating stimulus. It is possible that on working memory trials participants made a saccade toward

the to-be-remembered stimulus and were simply reporting the landing point of an adapted saccade independent of any mnemonic representation. To rule out this explanation, we ran two in-person studies with concurrent eye-tracking. These studies further enabled greater control of the experimental parameters (screen distance, stimulus size, etc.) than in prior online experiments and so would be expected to yield less variability across individuals. Experiment 4 presented stimuli in the right hemifield (matching Experiment 2). As Experiments 1-4 presented stimuli in the right hemifield, Experiment 5 presented stimuli in the left hemifield to ensure our results generalize to the entire visual field. Participants successfully maintained fixation for the period spanning the initial exogenous cue, the grating stimulus, and the 100 ms following the offset of the grating on the vast majority of trials (Experiment 4: 95.74 ± 1.25% of trials; Experiment 5: 94.87% ± 1.81% of trials; see Supplementary Fig. 3a and 4a for gaze density plots for each subject). This result indicates that the induced error on Att-error trials was indeed covert rather than overt and the shift in working memory recall cannot be attributed to eye movements to the attended hemifield on Att-error trials. Participants also maintained fixation during the period spanning the presentation of the to-be-remembered stimulus and 100 ms following the offset of the memory stimulus during adaptation block WM-fixed trials (Experiment 4: all adaptation blocks = 91.06% ± 2.35% of trials; last adaptation block = 92.27% ± 2.48% of trials; Experiment 5: all adaptation blocks = 93.18% ± 2.90% of trials; last adaptation block = 93.64% ± 3.07%; also see Supplementary Fig. 3b and 4b). Saccades following this interval would necessarily be memory-guided and cannot be attributed to visuomotor adaptation.

100% of participants exhibited some degree of adaptation (>5%) from the baseline period to the last adaptation block in both experiments (Experiment 4: –49.90% ± 6.23%, BF = 2.68×10^{45}; Experiment 5: –33.11% ± 1.02%, BF = 5.77×10^{22}). We found evidence in favor of no change in WM-fixed recall during the pre-adaptation block consisting entirely of working memory trials (Experiment 4: BF = 0.22; Experiment 5: BF = 0.13). We again observed strong evidence for de-adaptation following the offset of induced attentional errors (Experiment 4: 25.65% ± 7.64%, BF = 8,785,226,241; Experiment 5: 21.67% ± 8.27%, BF = 307,865,467). There was some evidence for a correlation in the magnitude of adaptation and de-adaptation across participants despite the small sample size (Experiment 4: $r(9) = –0.71$, BF = 4.37; Experiment 5: $r(9) = –0.85$, BF = 16.91). The double exponential decay model best fit the timecourse of adaptation in Experiment 4 (Linear ELPD = –58.4; Single Exponential ELPD = –30.0; Double Exponential ELPD = –24.4) and was slightly preferred in Experiment 5 (Linear ELPD = –42.7; Single Exponential ELPD = –29.3; Double Exponential ELPD = –26.0). We further found that adaptation was maximal on WM-random trials at the adapted location and adaptation transfer decreased with distance (Experiment 4: BF = 6.30; Linear Slope = 4.49% per degree of visual

angle, 95% CI [1.06%, 7.88%]; Experiment 5: BF = 47.72, Linear Slope = 6.68% per degree of visual angle, 95% CI [2.82% 10.71%]; Fig. 4b and d).

Discussion

The learning mechanisms underlying motor and cognitive control have traditionally been thought to be independent of one another. Across 5 experiments we demonstrate that errors in the covert allocation of attention were associated with a dramatic shift in spatial working memory representations in the direction of error. This adaptive shift could not be explained by attractive attentional biases or oculomotor processes. Rather, the effect was driven by covert sensory prediction errors, paralleling the learning mechanisms shown to underlie motor adaptation. Every time attention was exogenously drawn to a peripheral location, an oriented target stimulus was presented at a location shifted relative to the initial cued location. As a result, a spatial attention allocation error was induced on every trial. We demonstrate that participants adaptively shift working memory representations to counteract these errors. In other words, when presented with an object at a location associated with an attentional allocation error, participants will remember that object as being located closer to where attention should have been allocated to best discriminate the target stimulus. These findings provide novel evidence that working memory is subject to adaptive control mechanisms previously thought to be the sole domain of motor control.

Several studies have examined whether saccade adaptation has perceptual consequences.[22–25] It has been shown that spatial localization will shift in the direction of the induced oculomotor error. Many of these studies included a delay interval prior to the perceptual localization judgment, which indicates that these tasks possessed a working memory component and were not purely perceptual. The inclusion of a delay period in these studies indicates that saccade adaptation may also result in adaptation of working memory as a byproduct. A major distinction between these studies and the current study is how error was elicited. These prior studies elicited motor errors via overt eye movements, while we induced errors covertly while participants fixated on a central stimulus. Concurrent eye-tracking confirmed that participants were able to maintain fixation and that the induced errors were covert. Our results indicate that adaptive control of working memory can occur independently of the motor system.

Motor adaptation has been proposed to involve a mix of explicit and implicit mechanisms.[8–10,12] We find the scenario where our effect is entirely explained by an explicit learning strategy to be unlikely for several reasons. The induced error on Att-error trials was irrelevant to task performance. Participants were instructed to report the orientation

of the target stimulus and were simply told that a stimulus would appear at a peripheral location prior to the target appearing. The task instructions made no mention of the initial exogenous cue and the target appearing at different locations. Moreover, the working memory task was entirely independent of the attention task and participants were not provided feedback on their working memory performance. An explicit explanation of our findings would not only require participants to formulate a strategy based on an aspect of the design that was unrelated to their performance on attention trials, but to apply that strategy to an independent task where that strategy confers no performance benefit. Furthermore, if we assume that participants do transfer an explicit strategy between tasks, we would have expected to observe such a strategy in Experiment 3, in which the exogenous cue and target stimulus appeared at the same location. In this experiment, the participants were presented with multiple cues (exogenous cue and target) highlighting the behavioral relevance of the displaced location (relative to the stimulus location presented on WM-fixed trials). If participants were to apply an explicit strategy based on the spatial location of stimuli in the attention task to the independent working memory task, it would be mostly likely to be apparent in the experiment with consistent spatial cues. Yet, we observed no shift in working memory recall in this experiment. This finding indicates that any learning that occurred in the other experiments was driven by the induced spatial allocation error. Lastly, we would expect a purely explicit strategy would be expected to yield a step function in spatial recall across trials due to the sudden application of the strategy. Instead, we observe a gradual shift in recall over the adaptation phase of the experiment as attentional errors accumulate. This gradual shift was apparent in both the group average timecourse as well as in individual subjects (See Supplementary Fig. 1-2,6-7).

A wealth of prior research has investigated the close relationship between attention and working memory. Attention has been proposed to act as a gatekeeper to working memory.[13–19] Our results provide support for this hypothesis. This idea was difficult to test empirically due to the difficulty of disentangling attended and mnemonic location. Our adaptation paradigm enables us to experimentally dissociate attentional allocation and location of working memory target stimuli. Our results indicate that when attentional shifts are associated with allocation errors, working memory representations are biased in the same direction as the error. Covert attention can subdivided into two types: exogenous and endogenous attention. Exogenous attention is reflexive and stimulus-driven, while endogenous is voluntary and goal-driven.[26] One previous study provided some evidence that covert exogenous shifts of attention may undergo adaptive changes that look qualitatively similar to that seen in saccade adaptation.[27] However, the primary dependent measure indexing the locus of exogenous attention in this study was derived from self-report of an illusory line motion effect.[28] There is currently some debate as to whether this illusion reflects attention or rather a lower-level pre-

attentive sensory process.[29–33] As a result, it is unclear whether exogenous attention or a pre-attentive perceptual process was adapted in this study. To our knowledge, no prior study has examined whether endogenous attention shifts are subject to adaptive control. It is possible that our results can be explained by the transfer of adaptation of one form of attention (exogenous) to another form of attention (endogenous). Endogenous attention and working memory rely on similar neural substrates[34–39] and maintaining a spatial location in visual working memory has been likened to maintaining endogenous attention at a particular location.[18,40] Future studies will be needed to determine the exact relationship between working memory and endogenous attention and the degree to which each is subject to adaptive control.

Prior saccade adaptation studies have found graded transfer of adaptation to nearby spatial locations.[4,5,20] We also found evidence of adaptation transfer that decreased with distance from the adapted location. However, we only examined transfer along a single dimension (horizontal) and fixed error direction (inward). Our experiments were also underpowered in terms of the number of trials needed to fully determine the spatial specificity of the adaptation field. Further work will be needed to better characterize the selectivity of working memory adaptation across the visual field and assess the influence of eccentricity and error direction in greater detail.

Cerebellum has been extensively implicated in visuomotor adaptation.[41–43] Empirical studies and computational modeling of cerebellar function indicate that the cerebellum instantiates a forward model that predicts the sensory consequences of motor actions.[41,42,44–50] Recent evidence indicates that the cerebellum is also recruited by working memory and other cognitive paradigms.[51–62] Relative to cerebral cortex, the cerebellum is cytoarchitecturally homogenous[63,64] This has led to proposals that there exists a universal cerebellar transform or computation that is applied to the diverse array of inputs the cerebellum receives.[64–66] A major challenge to testing this hypothesis empirically has been translating well-established theories of cerebellar contributions to motor control to the cognitive domain. This has been difficult to test as task demands of motor and cognitive paradigms are often quite disparate. Here, we show that adaptive learning mechanisms known to be supported by the cerebellum[50,67] also appear to play a role in memory function. Our findings raise the possibility that the cerebellum may generally support adaptive control for both motor and cognitive processes. Yet, further research will be necessary to conclusively determine whether working memory adaptation relies on cerebellar function, and whether such a role differs from canonical working memory cortical regions such as the intraparietal sulcus or frontal eye fields.

Our findings open new avenues for exploring the extent to which learning mechanisms typically ascribed to motor control may contribute to cognitive function. These results suggest a more unified view of the brain's capacity for

adaptive control, where learning from errors acts as a central principle governing both motor and cognitive control, potentially mediated by common neural substrates such as the cerebellum. A greater appreciation for the role of error-based adaptive learning mechanisms in cognitive processes such as working memory has the potential to motivate the development of novel rehabilitative strategies for psychiatric and neurological disorders associated with executive function deficits.

Methods

Participants. 275 total healthy adult volunteers participated in this study. Experiments 1 (N = 94), 2 (N=85), and 3 (N=74) were conducted online. For these experiments, participants were recruited using Prolific (www.prolific.co) and the experimental paradigm was hosted on Pavlovia (pavlovia.org). We defined strict criteria for inclusion in further analysis (detailed below) resulting in sample sizes of 40 participants for Experiments 1-3. Prior to running any experiments, we ran a power analysis for a partial η^2 of 0.2, a power of 0.8, and an alpha of 0.05, which resulted in a required sample size of 35. As a result, we aimed to recruit 40 participants for each experiment. Experiments 4 (N=11) and 5 (N=11) were conducted in-person on the University of Michigan campus. All research protocols were approved by the Health Sciences and Behavioral Sciences Institutional Review Board at the University of Michigan. All participants gave written informed consent. Online participants were paid $10/hr for their participation. In-person participants were paid $15/hr for their participation. In-person participants were recruited from University of Michigan and the surrounding community. All participants possessed normal or corrected-to-normal vision.

Stimuli and Experimental Paradigm. Stimuli were generated and presented using Python with the PsychoPy software package (Pierce et al., 2019). The task consisted of 3 trial types: exogenous attention back-step trials (Att-error), random working memory trials (WM-random), and fixed working memory trials (WM-fixed). Trials were separated into 5 blocks. In Experiment 1, all blocks were identical and consisted of 220 Att-error trials, 20 WM-random trials, and 20 WM-fixed trials. During these blocks, participants were presented with 5 or 6 Att-error trials followed by either a WM-random or WM-fixed trial. Online experiments defined stimulus size and location using normalized 'height' units, which scale stimuli relative to the height of the participant's screen (see https://www.psychopy.org/general/units.html). For a standard widescreen (16:10 aspect ratio) the bottom left of the screen has the coordinates [–0.8, –0.5] and the top right of the screen has the coordinates [+0.8,+0.5]. Att-error trials presented an exogenous cue in the right hemifield (presented at [+0.5,0]; diameter = 0.02 height units) along the horizontal meridian for 116.67 ms (7 frames at 60 Hz) (Fig. 1a). The presentation time was selected based on a previous study that estimated the mean shift time for exogenous attention to be 116 ms.[27]

Immediately following the offset of the exogenous attention cue, participants were presented with a line within a circle (diameter = 0.02 height units) that was randomly oriented at either 45° or 135° for 100 ms. The oriented line stimulus was displaced inwards relative to the initial exogenous cue (presented at [+0.33,0]). By surreptitiously shifting the to-be-attended location we induced an attentional allocation error on each trial. Participants were instructed to use the left and right arrow keys to indicate whether the line stimulus was oriented at 45° or 135° (right – 45°; left – 135°). WM-random and WM-fixed trials presented a circular stimulus (diameter = 0.02 height units) for 100 ms (Figure 1B). On WM-random trials, the stimulus could appear anywhere along the horizontal meridian between [+0.22, 0] and [+0.7, 0]. On WM-fixed trials, the stimulus always appeared at the same location as the initial exogenous cue on Att-error trials (i.e. [+0.5, 0]). Following a 500 ms delay interval, participants were presented with a slider stimulus and instructed to click the location on the line where the dot stimulus appeared. Once they clicked on the line a triangular marker appeared. Participants were able to drag this marker with their mouse to adjust their response. The slider spanned from [+0.17, 0] to [+0.75, 0] to avoid potential edge effects. Instructions emphasized the importance of fixating on the central dot stimulus and keeping head-to-screen relative position and distance constant.

Experiment 2 changed the trial sequence while keeping all other within-trial aspects of stimulus timing and appearance identical to Experiment 1. To account for potential sequential biases in spatial eccentricity recall with the performance of repeated working memory trials and to establish a pre-adaptation baseline, Experiment 2 included a block of trials consisting entirely of working memory trials (75 WM-random and 25 WM-fixed) prior to the adaptation blocks. To investigate the rate of de-adaptation, Experiment 2 also presented another working memory-only block at the end of the experiment following the adaptation period. To limit the total duration of the experiment we reduced the number of intervening adaptation blocks to three (660 Att-error trials, 60 WM-fixed trials, and 60 WM-random trials).

Experiment 3 investigated whether a shift in spatial working memory recall can be attributed to mechanisms fundamentally different from the mechanisms governing motor adaptation. It is possible that repeatedly attending a particular location biases subsequent working memory towards that location. To examine whether an error signal is necessary to shift spatial working memory recall, we presented the initial exogenous cue at the same location as the subsequent oriented line stimulus (i.e. [+0.33, 0]). WM-fixed trials were identical to prior experiments with the stimulus appearing at [+0.5, 0]. If we observe the same shift in working memory representations it would suggest that sensory prediction errors do not drive this change and that the observed shift is unlikely to reflect the same phenomenon observed in motor adaptation tasks. Rather, it would suggest that the observed shift reflects another form of bias such as attentional

attraction to a behaviorally relevant location. If we observe no shift in spatial working memory recall it would indicate that any learning observed in Experiments 1 and 2 is error-driven and can be likened to motor adaptation.

Experiments 4 and 5 were conducted in-person with concurrent eye-tracking (preprocessing and analysis of eye-tracking data detailed below). Gaze position was monocularly monitored and recorded from the right eye with a sampling rate of 1000 Hz using a desktop-mounted EyeLink 1000 Plus eye-tracker (SR Research). To minimize head motion and control viewing distance, participants performed the experiment using a chin rest positioned 85 cm from the screen. A 9-point calibration procedure was performed prior to the beginning of the experiment as well as between each block. Stimulus size and location were defined in degrees of visual angle. Att-error trials either presented the exogenous cue in the right hemifield (Experiment 4; [+9°, 0°]; diameter = 0.3°) or the left hemifield (Experiment 5; [–9°, 0°]; diameter = 0.3°) along the horizontal meridian. Immediately following the offset of the exogenous attention cue, participants were presented with a sine wave grating stimulus (diameter = 0.3°; spatial frequency = 10 cycles/°; 100% contrast; raised cosine mask; 20% of stimulus diameter devoted to the raised cosine mask) at [6°, 0°] (Experiment 4) or [–6°, 0°] (Experiment 5) that was randomly oriented at either 45° or 135° for 100 ms. WM-random and WM-fixed trials presented a circular stimulus (diameter = 0.3°) for 100 ms followed by a 500 ms delay interval (Fig. 1b). On WM-random trials, the stimulus could appear anywhere along the horizontal meridian between [±4°, 0] and [±11°, 0]. On WM-fixed trials, the stimulus appeared at the same location as the initial exogenous cue on Att-error trials (i.e. [±9°, 0]). The probe slider stimulus spanned from [±3°, 0] to [±12°, 0] to avoid potential edge effects.

Online exclusion criteria. We defined strict *a priori* exclusion criteria for online experiments. In Experiment 1, participants were excluded if they responded on less than 66.67% of any trial type. For Experiments 2 and 3, we increased this criterion to a 75% response rate. Additionally, any participants who performed with less than 66.67% accuracy on Att-error trials and/or possessed a mean absolute error greater than 0.15 normalized height units on WM-random trials (determined by performing simulations of mean absolute error for random slider responses) were excluded from further analysis. We included the following two self-report questions at the end of the experiment to determine if participants potentially exhibited behavior that would be expected to eliminate or reduce the hypothesized effect: "How much did your head move relative to the screen over the course of the experiment”? (Possible Answers: None; Some - 0-6 inches; Quite a bit - 6-12 inches; An extreme amount - 12+ inches) and "What percentage of the time were you able to keep your eyes focused on the center of the display?” (Possible Answers: 0%-100%). If participants responded "Quite a bit" or “An extreme amount” for the head movement question or <70% for the eye movement question they were excluded from

further analysis. We further excluded participants if any one of the breaks between blocks was longer than 10 minutes. We realized during analysis that 2 participants were included in Experiment 1 analyses that had responded "Quite a bit" for the head movement question while satisfying all other criteria. Removing these participants does not change any of the inferences made with the full sample of 40. Note that all of these exclusion criteria are independent of performance on WM-fixed trials, which were used to compute our primary outcome (adaptation magnitude).

Statistical Analysis. All analysis was performed with R (R Version 4.3.1). To assess the difference in spatial recall between the 1st block (Experiment 1: 1st adapt block; Experiments 2-5: pre-adapt block) and the last adaptation block (Experiment 1: 5th adaptation block; Experiments 2-5: 3rd adaptation block) we used the BayesFactor package[68] to fit a hierarchical linear model and compute Bayes Factors (BF). We compared a full model that included the effects of block and subject variability to an intercept-only model which accounted for random effects due to subject variability alone. The models were specified as follows:

$$M_{S+B}: y = \mu 1 + \sigma(X_s\beta_s + X_B\beta_B) + \epsilon$$

$$M_S: y = \mu 1 + \sigma X_s\beta_s + \epsilon$$

Where y is a vector of N observations, μ is a grand mean parameter, 1 is a column vector of length N consisting entirely of ones, X_s is a design matrix of size $N \times m$ subjects, X_B is a design matrix of size $N \times (n\text{-}1)$ blocks, and β_s and β_B are vectors of standardized effects for subject and block. Effects were standardized relative to the standard deviation of the error (σ).

A Jeffreys prior[69] was placed on the grand mean μ and the variance σ^2, while independent scaled inverse-chi-square priors with one degree of freedom were set on the *g*-prior parameters characterizing the subject and block effects.[70,71] The scale parameter for the random subject effect was set to 1, which is appropriate for medium to large-sized effects that are not of primary interest.[71] The scale parameter for the fixed block effect was set to 0.5, which indicates that *a priori* we expect a medium effect size (BayesFactor package default). Critically, all reported effects were robust to this prior definition.

*BF*s were computed by integrating the likelihood with respect to the priors. The full model *BF* (BF_{S+B}) was computed by specifying block and subject as predictors, with subject treated as a random effect. The intercept-only model Bayes factor (BF_S) included only the subject as a random effect. The ratio BF_{S+B} / BF_S provides a measure of the evidence for the effect of block while accounting for subject variability.

To examine the difference in spatial recall following the cessation of covert attentional errors, we fit another hierarchical linear model to assess the degree of de-adaptation between the final adaptation block and the post-adaptation block for Experiments 2-5. We again assessed the evidence for a block effect by computing the ratio BF_{S+B} / BF_S which controls for variance associated with subject.

To test for any trends in spatial recall in the pre-adaptation period (Experiments 2-6) in the absence of covert attentional errors we additionally fit a linear model that included a fixed effect of trial and a random subject effect. We report the *BF* from this fit as well as the estimated slope.

To characterize the timecourse of adaptation, we additionally fit 3 continuous models: a linear model, a single exponential decay model, and a double exponential decay model. Single and double exponential decay models have been used extensively to characterize the timecourse of visuomotor adaptation (Fujita et al., 2002). The single exponential was defined using the following formula:

$$y_{recall} = \alpha \times 2^{\frac{-t}{\tau}} + \beta$$

Where y_{recall} represents the recalled location along the horizontal meridian for each trial, α represents the absolute change in recall, *t* represents the absolute trial number including all trial types (Att-error, WM-fixed, and WM-random), τ represents the half-life (i.e. number of trials it takes for the decay to reach $\alpha/2$), and β represents the asymptote.

It has been proposed that motor adaptation relies on two memory systems characterized by different rates of learning.[21] To account for multiple timescales of memory in adaptive control we additionally fit a double exponential decay model. This model was defined using the following formula:

$$y_{recall} = (\alpha_1 \times 2^{\frac{-t}{\tau_1}}) + (\alpha_2 \times 2^{\frac{-t}{\tau_2}}) + \beta$$

Where α_1 and α_2 represent the amplitudes for the fast and slow learning processes, and τ_1 and τ_2 represent the rates for the two learning processes.

For experiments 2-6, which included a pre-adaptation baseline period, all pre-adapt trials were labeled as trial 0. A posterior distribution over possible parameter values for each model was sampled using Markov chain Monte Carlo (MCMC) sampling implemented in *rstan*[72] (Version 2.21.8) via the brms package[73,74] (Version 2.19.0). We then used the *loo* package[75,76] (Version 2.6.0) to perform model comparison. The *loo* package computes an approximate leave-one-out cross-validation (LOO) metric, the expected pointwise log predictive density (ELPD), using Pareto-Smoothed Importance Sampling (PSIS).[75] We compared the ELPD between models. If the ELPD difference between two models was less than 4

the difference between models was considered negligible and we used the simpler model for plots and reporting (e.g. single exponential decay model rather than the double exponential decay model).[77]

To examine the transfer of adaptation to nearby locations in space, we binned WM-random trials based on memory stimulus location. Experiments 1-2 used the following standardized screen unit bins: (–Inf, 0.15], (0.15, 0.25], (0.25, 0.35], (0.35, 0.45], (0.45, 0.55], (0.55, 0.65], and (0.65, Inf], while Experiments 4-5 used the following degrees of visual angle unit bins: (–Inf, 4.5°], (4.5°, 5.5°], (5.5°, 6.5°], (6.5°, 7.5°], (7.5°, 8.5°], (8.5°, 9.5°], (9.5°, 10.5°], and (10.5°, Inf]; Experiment 5 presented stimuli in the left hemifield so the sign of the bins was reversed (e.g. (–9.5°, –8.5°]). Bin definitions were chosen to maximize the number of trials within each bin for each subject while maintaining location specificity. To examine the transfer of adaptation to nearby locations, we fit a Bayesian hierarchical linear regression model to examine the relationship between working memory recall and distance from the adapted location.

Eye tracking analysis. Eye-tracking data were first converted from edf to asc format. Data were then parsed, preprocessed, and analyzed using a combination of functions from the *GazeR* R package[78] and custom R code. Eye blinks were detected and interpolated (±100 ms around detected blinks) using a linear interpolation procedure. We then performed offline drift correction by computing the median gaze position for the first 200 ms of each trial (100 ms trial start cue + 100 ms fixation) and then subtracting this value from the start and end points of all saccades for that trial. The onset and offset of saccades were detected using standard EyeLink parameters (velocity threshold of 30°/s, acceleration threshold 8000 °/sec^2, 0.1° displacement threshold). For Att-error trials, we examined whether participants' gaze deviated from fixation more than 1° towards the stimulus (right hemifield for experiment 4 and left hemifield for experiment 5) during the epoch of presentation comprising the initial exogenous cue, the shifted grating stimulus, and 100 ms following the offset of the grating stimulus. For working memory trials, we examined whether participants broke fixation during the presentation of the to-be-remembered stimulus and the 100 ms following the offset of the memoranda.

Data Availability

The data supporting the findings of this study are available at https://osf.io/egskw/.

Code Availability

The analysis code supporting the findings of this study is available at https://github.com/brissend/WM_adapt.

References

1. Shadmehr, R., Smith, M. A. & Krakauer, J. W. Error Correction, Sensory Prediction, and Adaptation in Motor Control. *Neuroscience* **33**, 89–108 (2010).

2. McLaughlin, S. C. Parametric adjustment in saccadic eye movements. *Percept Psychophys* **2**, 359–362 (1967).

3. Deubel, H., Wolf, W. & Hauske, G. Adaptive gain control of saccadic eye movements. *Hum. Neurobiol.* **5**, 245–53 (1986).

4. Frens, M. A. & Opstal, A. J. van. Transfer of short-term adaptation in human saccadic eye movements. *Exp. Brain Res.* **100**, 293–306 (1994).

5. Straube, A., Fuchs, A. F., Usher, S. & Robinson, F. R. Characteristics of Saccadic Gain Adaptation in Rhesus Macaques. *J. Neurophysiol.* **77**, 874–895 (1997).

6. Hopp, J. J. & Fuchs, A. F. The characteristics and neuronal substrate of saccadic eye movement plasticity. *Prog. Neurobiol.* **72**, 27–53 (2004).

7. Watanabe, S., Ogino, S., Nakamura, T. & Koizuka, I. Saccadic adaptation in the horizontal and vertical directions in normal subjects. *Auris Nasus Larynx* **30**, 41–45 (2003).

8. Mazzoni, P. & Krakauer, J. W. An Implicit Plan Overrides an Explicit Strategy during Visuomotor Adaptation. *J Neurosci* **26**, 3642–3645 (2006).

9. Taylor, J. A., Krakauer, J. W. & Ivry, R. B. Explicit and Implicit Contributions to Learning in a Sensorimotor Adaptation Task. *J. Neurosci.* **34**, 3023–3032 (2014).

10. McDougle, S. D., Bond, K. M. & Taylor, J. A. Explicit and Implicit Processes Constitute the Fast and Slow Processes of Sensorimotor Learning. *J. Neurosci.* **35**, 9568–9579 (2015).

11. Kooij, K. van der, Wijdenes, L. O., Rigterink, T., Overvliet, K. E. & Smeets, J. B. J. Reward abundance interferes with error-based learning in a visuomotor adaptation task. *PLoS ONE* **13**, e0193002 (2018).

12. Albert, S. T. *et al.* An implicit memory of errors limits human sensorimotor adaptation. *Nat Hum Behav* 1–15 (2021) doi:10.1038/s41562-020-01036-x.

13. Awh, E., Vogel, E. K. & Oh, S.-H. Interactions between attention and working memory. *Neuroscience* **139**, 201–208 (2006).

14. Schmidt, B. K., Vogel, E. K., Woodman, G. F. & Luck, S. J. Voluntary and automatic attentional control of visual working memory. *Percept. Psychophys.* **64**, 754–763 (2002).

15. Cowan, N. & Morey, C. C. Visual working memory depends on attentional filtering. *Trends Cogn. Sci.* **10**, 139–141 (2006).

16. Chun, M. M. & Turk-Browne, N. B. Interactions between attention and memory. *Curr. Opin. Neurobiol.* **17**, 177–184 (2007).

17. McNab, F. & Klingberg, T. Prefrontal cortex and basal ganglia control access to working memory. *Nat. Neurosci.* **11**, 103–107 (2008).

18. Kiyonaga, A. & Egner, T. Working memory as internal attention: Toward an integrative account of internal and external selection processes. *Psychon. Bull. Rev.* **20**, 228–242 (2013).

19. Fougnie, D. & Marois, R. Attentive tracking disrupts feature binding in visual working memory. *Vis. Cogn.* **17**, 48–66 (2009).

20. Noto, C. T., Watanabe, S. & Fuchs, A. F. Characteristics of Simian Adaptation Fields Produced by Behavioral Changes in Saccade Size and Direction. *J Neurophysiol* **81**, 2798–2813 (1999).

21. Smith, M. A., Ghazizadeh, A. & Shadmehr, R. Interacting Adaptive Processes with Different Timescales Underlie Short-Term Motor Learning. *Plos Biol* **4**, e179 (2006).

22. Bahcall, D. O. & Kowler, E. Illusory shifts in visual direction accompany adaptation of saccadic eye movements. *Nature* **400**, 864–866 (1999).

23. Hernandez, T. D., Levitan, C. A., Banks, M. S. & Schor, C. M. How does saccade adaptation affect visual perception? *J Vision* **8**, 3–3 (2008).

24. Schnier, F., Zimmermann, E. & Lappe, M. Adaptation and mislocalization fields for saccadic outward adaptation in humans. *J Eye Movement Res* **3**, (2010).

25. Cheviet, A. *et al.* Cerebellar Signals Drive Motor Adjustments and Visual Perceptual Changes during Forward and Backward Adaptation of Reactive Saccades. *Cereb. Cortex* **32**, 3896–3916 (2022).

26. Carrasco, M. Visual attention: The past 25 years. *Vis. Res.* **51**, 1484–1525 (2011).

27. McFadden, S. A., Khan, A. & Wallman, J. Gain adaptation of exogenous shifts of visual attention. *Vision Res* **42**, 2709–2726 (2002).

28. Hikosaka, O., Miyauchi, S. & Shimojo, S. Visual attention revealed by an illusion of motion. *Neurosci. Res.* **18**, 11–18 (1993).

29. Downing, P. E. & Treisman, A. M. The Line-Motion Illusion: Attention or Impletion? *J Exp Psychology Hum Percept Perform* **23**, 768–779 (1997).

30. Tse, P., Cavanagh, P. & Nakayama, K. High-Level Motion Processing. 244–261 (1998) doi:10.7551/mitpress/3495.003.0011.

31. Schmidt, W. C. Endogenous Attention and Illusory Line Motion Reexamined. *J. Exp. Psychol.: Hum. Percept. Perform.* **26**, 980–996 (2000).

32. Christie, J. & Klein, R. M. Does attention cause illusory line motion? *Percept. Psychophys.* **67**, 1032–1043 (2005).

33. Ono, F., Yamada, Y., Takahashi, K., Sasaki, K. & Ariga, A. Backward illusory line motion: Visual motion perception can be influenced by retrospective stimulation. *J. Vis.* **23**, 6 (2023).

34. Awh, E. & Jonides, J. Overlapping mechanisms of attention and spatial working memory. *Trends Cogn. Sci.* **5**, 119–126 (2001).

35. Corbetta, M. & Shulman, G. L. Control of goal-directed and stimulus-driven attention in the brain. *Nat. Rev. Neurosci.* **3**, 201–215 (2002).

36. Jerde, T. A., Merriam, E. P., Riggall, A. C., Hedges, J. H. & Curtis, C. E. Prioritized Maps of Space in Human Frontoparietal Cortex. *J Neurosci* **32**, 17382–17390 (2012).

37. Sprague, T. C. & Serences, J. T. Attention modulates spatial priority maps in the human occipital, parietal and frontal cortices. *Nat. Neurosci.* **16**, 1879–1887 (2013).

38. Panichello, M. F. & Buschman, T. J. Shared mechanisms underlie the control of working memory and attention. *Nature* **592**, 601–605 (2021).

39. Zhou, Y., Curtis, C. E., Sreenivasan, K. K. & Fougnie, D. Common Neural Mechanisms Control Attention and Working Memory. *J. Neurosci.* **42**, 7110–7120 (2022).

40. Chun, M. M. Visual working memory as visual attention sustained internally over time. *Neuropsychologia* **49**, 1407–1409 (2011).

41. Wolpert, D. M., Miall, R. C. & Kawato, M. Internal models in the cerebellum. *Trends Cogn Sci* **2**, 338–347 (1998).

42. Bastian, A. J. Learning to predict the future: the cerebellum adapts feedforward movement control. *Curr. Opin. Neurobiol.* **16**, 645–649 (2006).

43. Tzvi, E., Loens, S. & Donchin, O. Mini-review: The Role of the Cerebellum in Visuomotor Adaptation. *Cerebellum* **21**, 306–313 (2022).

44. Miall, R. C. & Wolpert, D. M. Forward Models for Physiological Motor Control. *Neural Networks* **9**, 1265–1279 (1996).

45. Imamizu, H. *et al.* Human cerebellar activity reflecting an acquired internal model of a new tool. *Nature* **403**, 192–195 (2000).

46. Tseng, Y., Diedrichsen, J., Krakauer, J. W., Shadmehr, R. & Bastian, A. J. Sensory Prediction Errors Drive Cerebellum-Dependent Adaptation of Reaching. *J. Neurophysiol.* **98**, 54–62 (2007).

47. Therrien, A. S. & Bastian, A. J. Cerebellar damage impairs internal predictions for sensory and motor function. *Curr Opin Neurobiol* **33**, 127–133 (2015).

48. Schlerf, J., Ivry, R. B. & Diedrichsen, J. Encoding of Sensory Prediction Errors in the Human Cerebellum. *J. Neurosci.* **32**, 4913–4922 (2012).

49. Tanaka, H., Ishikawa, T., Lee, J. & Kakei, S. The Cerebro-Cerebellum as a Locus of Forward Model: A Review. *Front. Syst. Neurosci.* **14**, 19 (2020).

50. Raymond, J. L. & Medina, J. F. Computational Principles of Supervised Learning in the Cerebellum. *Annu. Rev. Neurosci.* **41**, 233–253 (2018).

51. Allen, G., Buxton, R. B., Wong, E. C. & Courchesne, E. Attentional Activation of the Cerebellum Independent of Motor Involvement. *Science* **275**, 1940–1943 (1997).

52. Chen, S. H. A. & Desmond, J. E. Cerebrocerebellar networks during articulatory rehearsal and verbal working memory tasks. *Neuroimage* **24**, 332–338 (2005).

53. Chen, S. H. A. & Desmond, J. E. Temporal dynamics of cerebro-cerebellar network recruitment during a cognitive task. *Neuropsychologia* **43**, 1227–1237 (2005).

54. Kirschen, M. P., Chen, S. H. A., Schraedley-Desmond, P. & Desmond, J. E. Load- and practice-dependent increases in cerebro-cerebellar activation in verbal working memory: an fMRI study. *Neuroimage* **24**, 462–472 (2005).

55. Stoodley, C. J., Valera, E. M. & Schmahmann, J. D. Functional topography of the cerebellum for motor and cognitive tasks: An fMRI study. *Neuroimage* **59**, 1560–1570 (2012).

56. Brissenden, J. A., Levin, E. J., Osher, D. E., Halko, M. A. & Somers, D. C. Functional Evidence for a Cerebellar Node of the Dorsal Attention Network. *J Neurosci Official J Soc Neurosci* **36**, 6083–96 (2016).

57. Brissenden, J. A. *et al.* Topographic Cortico-cerebellar Networks Revealed by Visual Attention and Working Memory. *Curr Biol* **28**, 3364-3372.e5 (2018).

58. Brissenden, J. A., Tobyne, S. M., Halko, M. A. & Somers, D. C. Stimulus-Specific Visual Working Memory Representations in Human Cerebellar Lobule VIIb/VIIIa. *J Neurosci* JN-RM-1253-20 (2020) doi:10.1523/jneurosci.1253-20.2020.

59. Sokolov, A. A., Miall, R. C. & Ivry, R. B. The Cerebellum: Adaptive Prediction for Movement and Cognition. *Trends Cogn Sci* **21**, 313–332 (2017).

60. Guell, X., Schmahmann, J. D., Gabrieli, J. D. & Ghosh, S. S. Functional gradients of the cerebellum. *Elife* **7**, e36652 (2018).

61. King, M., Hernandez-Castillo, C. R., Poldrack, R. A., Ivry, R. B. & Diedrichsen, J. Functional boundaries in the human cerebellum revealed by a multi-domain task battery. *Nat Neurosci* **22**, 1371–1378 (2019).

62. Hayter, A. L., Langdon, D. W. & Ramnani, N. Cerebellar contributions to working memory. *Neuroimage* **36**, 943–954 (2007).

63. Itō, M. *The Cerebellum and Neural Control*. (Raven Press, 1984).

64. Ramnani, N. The primate cortico-cerebellar system: anatomy and function. *Nat Rev Neurosci* **7**, 511–522 (2006).

65. Schmahmann, J. D. The role of the cerebellum in affect and psychosis. *J Neurolinguist* **13**, 189–214 (2000).

66. Ito, M. Control of mental activities by internal models in the cerebellum. *Nat Rev Neurosci* **9**, 304–313 (2008).

67. Herzfeld, D. J., Kojima, Y., Soetedjo, R. & Shadmehr, R. Encoding of error and learning to correct that error by the Purkinje cells of the cerebellum. *Nat Neurosci* **21**, 736–743 (2018).

68. Morey, R. & Rouder, J. N. BayesFactor: Computation of Bayes Factors for Common Designs. https://cran.radicaldevelop.com/web/packages/BayesFactor/BayesFactor.pdf (2023).

69. Jeffreys, H. An invariant form for the prior probability in estimation problems. *Proc. R. Soc. Lond. Ser. A Math. Phys. Sci.* **186**, 453–461 (1946).

70. Zellner, A. & Siow, A. Posterior odds ratios for selected regression hypotheses. *Trab. Estad. Y Investig. Oper.* **31**, 585–603 (1980).

71. Rouder, J. N., Morey, R. D., Speckman, P. L. & Province, J. M. Default Bayes factors for ANOVA designs. *J Math Psychol* **56**, 356–374 (2012).

72. Stan Development Team. *RStan: The R Interface to Stan*. (2023).

73. Bürkner, P.-C. Advanced Bayesian Multilevel Modeling with the R Package brms. *The R Journal* **10**, 395–411 (2018).

74. Bürkner, P.-C. brms: An R Package for Bayesian Multilevel Models Using Stan. *Journal of Statistical Software* **80**, 1–28 (2017).

75. Vehtari, A., Gelman, A. & Gabry, J. Practical Bayesian model evaluation using leave-one-out cross-validation and WAIC. *Stat. Comput.* **27**, 1413–1432 (2017).

76. Vehtari, A. *et al.* loo: Efficient Leave-One-Out Cross-Validation and WAIC for Bayesian Models. *R package version 2.6.0* https://cran.r-project.org/web/packages/loo/loo.pdf (2023).

77. Sivula, T., Magnusson, M., Matamoros, A. A. & Vehtari, A. Uncertainty in Bayesian Leave-One-Out Cross-Validation Based Model Comparison. (2020).

78. Geller, J., Winn, M. B., Mahr, T. & Mirman, D. GazeR: A Package for Processing Gaze Position and Pupil Size Data. *Behav Res Methods* **52**, 2232–2255 (2020).

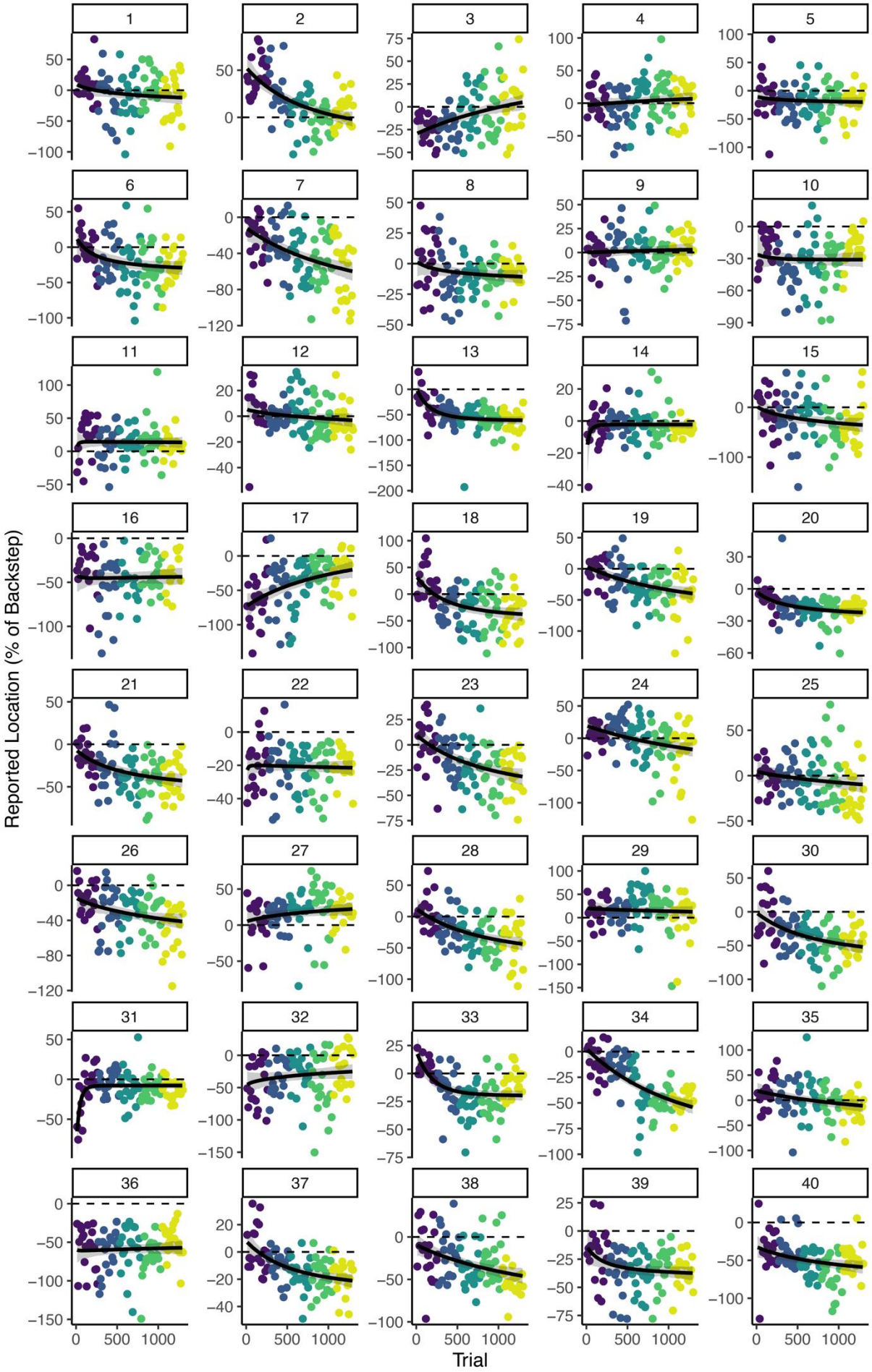
Reported Location (% of Backstep)
Trial
1
2
3
4
5
6
7
8
9
10
11
12
13
14
15
16
17
18
19
20
21
22
23
24
25
26
27
28
29
30
31
32
33
34
35
36
37
38
39
40

Supplementary Figure 1. Experiment 1 individual participant working memory recall timecourses. Individual data points represent trial recall location (N=40) as a percentage of the backstep size on Att-error trials for each WM-fixed trial. The target stimulus appeared at the same location in all trials shown (i.e. 0%). The *x*-axis represents the absolute trial number across all trial types (Att-error, WM-random, and WM-fixed). Color denotes block number. Black lines in each plot represent the mean of an exponential decay model posterior predictive distribution and the shaded areas represent the 95% credible interval of the expected values of the posterior predictive distribution.

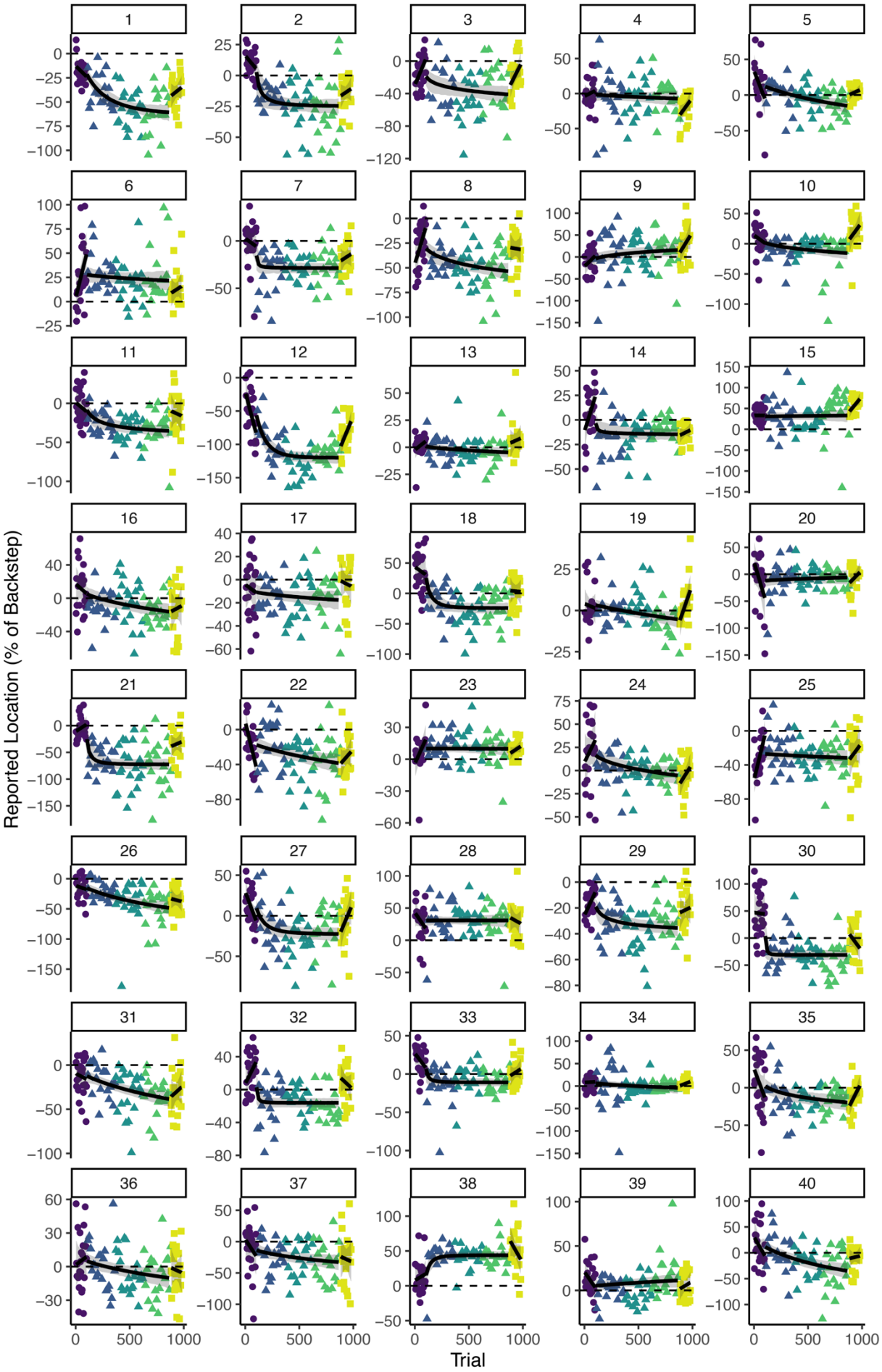
Reported Location (% of Backstep)
Trial
1
2
3
4
5
6
7
8
9
10
11
12
13
14
15
16
17
18
19
20
21
22
23
24
25
26
27
28
29
30
31
32
33
34
35
36
37
38
39
40
0
500
1000

Supplementary Figure 2. Experiment 2 individual participant working memory recall timecourses. Individual data points represent trial recall location (N=40) as a percentage of the backstep size on Att-error trials for each WM-fixed trial. The target stimulus appeared at the same location in all trials shown (i.e. 0%). The *x*-axis represents the absolute trial number across all trial types (Att-error, WM-random, and WM-fixed). Color denotes block number and shape represents the phase of the experiment. The black lines spanning the pre- and post-adapt phases represent the mean of a linear model posterior predictive distribution, while the black line spanning the adapt phase is the mean of an exponential decay model posterior predictive distribution. The shaded area denotes the 95% credible interval of the expected value distribution for each model.

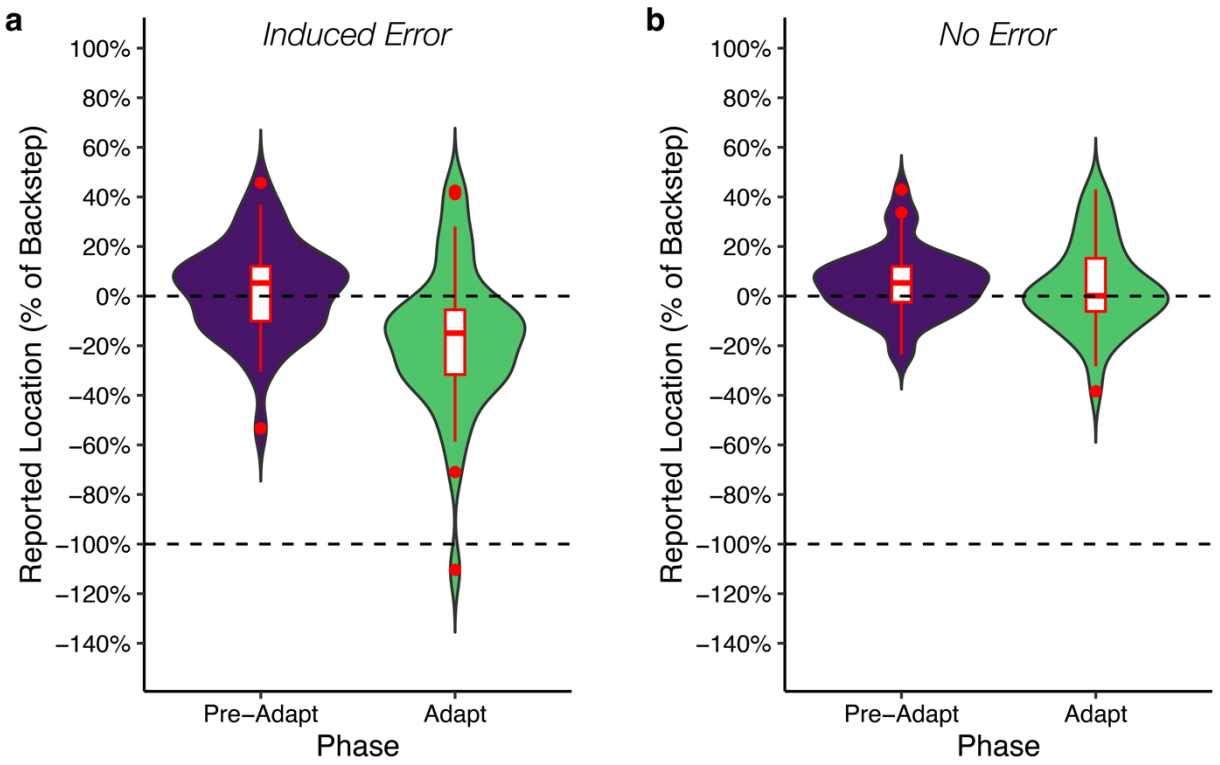

Supplementary Figure 3. Working memory adaptation is dependent on induced error. a, Repeatedly inducing errors in the covert allocation of spatial attention is associated with an adaptive shift in working memory recall. Violin and boxplots summarize the distribution of mean WM-fixed recall across subjects for the pre-adapt block and the last block of the adaptation phase in Experiment 2. **b,** Repeatedly drawing attention to a nearby location without inducing an error does not lead to a shift in working memory recall. Violin and boxplots summarize the distribution of mean WM-fixed recall across subjects for the pre-adapt block and the last block of the adaptation phase in Experiment 3. Boxplots show median (bar), quartiles (boxes), range (whiskers), and outliers (circles).

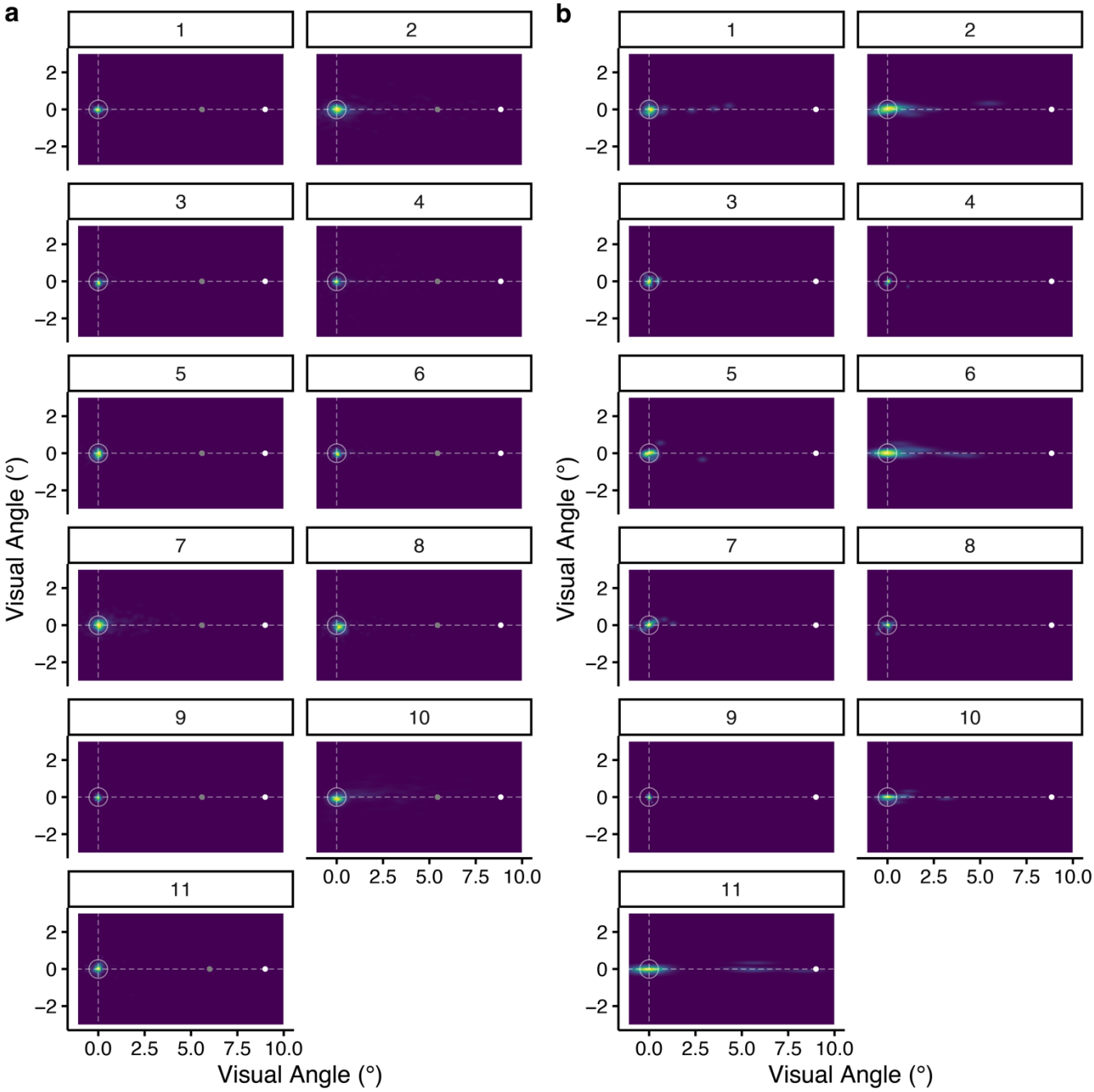

Supplementary Figure 4. Experiment 4 individual participant gaze tracking. a, Illustration of experiment 4 gaze data for Att-error trials. Heatmaps show gaze density for each participant over trials averaged over the period spanning the presentation of the initial cue, target stimulus, and the 100 ms following the offset of the target stimulus. Dashed lines denote the horizontal and vertical meridians intersecting with the center of the display. White circle denotes a 1° of visual angle radius ring around central fixation. The white disc shows the location of the initial exogenous cue (color is for illustration purposes only; stimulus was black in actual experiment). Circular sine wave grating depicted at the location of the to-be-discriminated target stimulus. Densities are scaled to a maximum of 1 for each participant. **b,** Illustration of gaze data for WM-fixed trials over the last block of the adaptation period. Heatmaps show gaze density for each participant averaged over the period spanning the presentation of the to-be-remembered stimulus and the 100 ms following the offset of the sample stimulus. The white disc depicts the location of the WM-fixed sample stimulus.

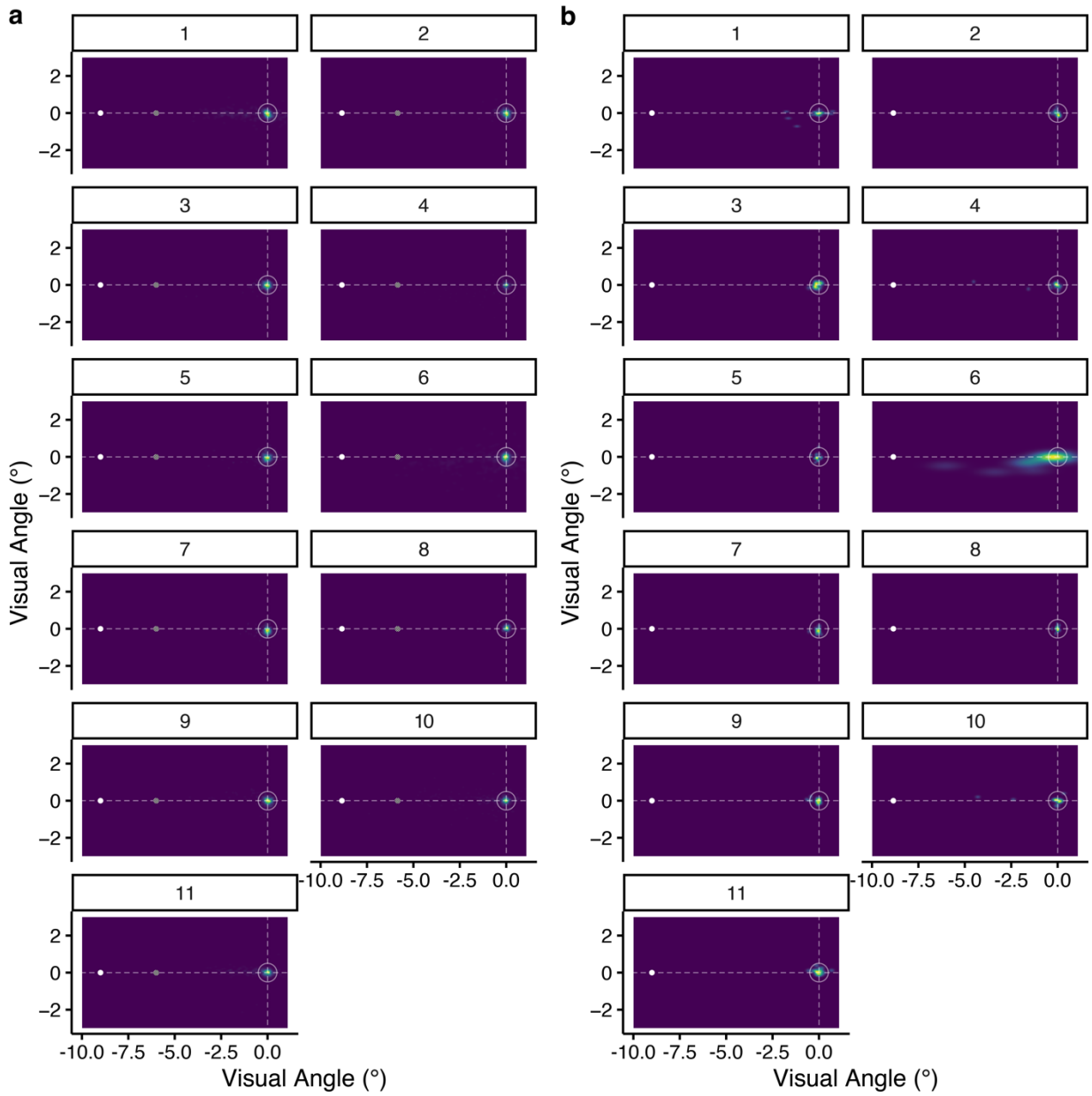

Supplementary Figure 5. Experiment 5 individual participant gaze tracking. a, Illustration of experiment 5 gaze data for Att-error trials. Heatmaps show gaze density for each participant averaged over the period spanning the presentation of the initial cue, target stimulus, and the 100 ms following the offset of the target stimulus. Dashed lines denote the horizontal and vertical meridians intersecting with the center of the display. White circle denotes a 1° of visual angle radius ring around central fixation. The white disc shows the location of the initial exogenous cue (color is for illustration purposes only; stimulus was black in actual experiment). Circular sine wave grating depicted at the location of the to-be-discriminated target stimulus. Densities are scaled to a maximum of 1 for each participant. **b,** Illustration of gaze data for WM-fixed trials over the last block of the adaptation period. Heatmaps show gaze density for each participant averaged over the period spanning the presentation of the to-be-remembered stimulus and the 100 ms following the offset of the sample stimulus. The white disc depicts the location of the WM-fixed sample stimulus.

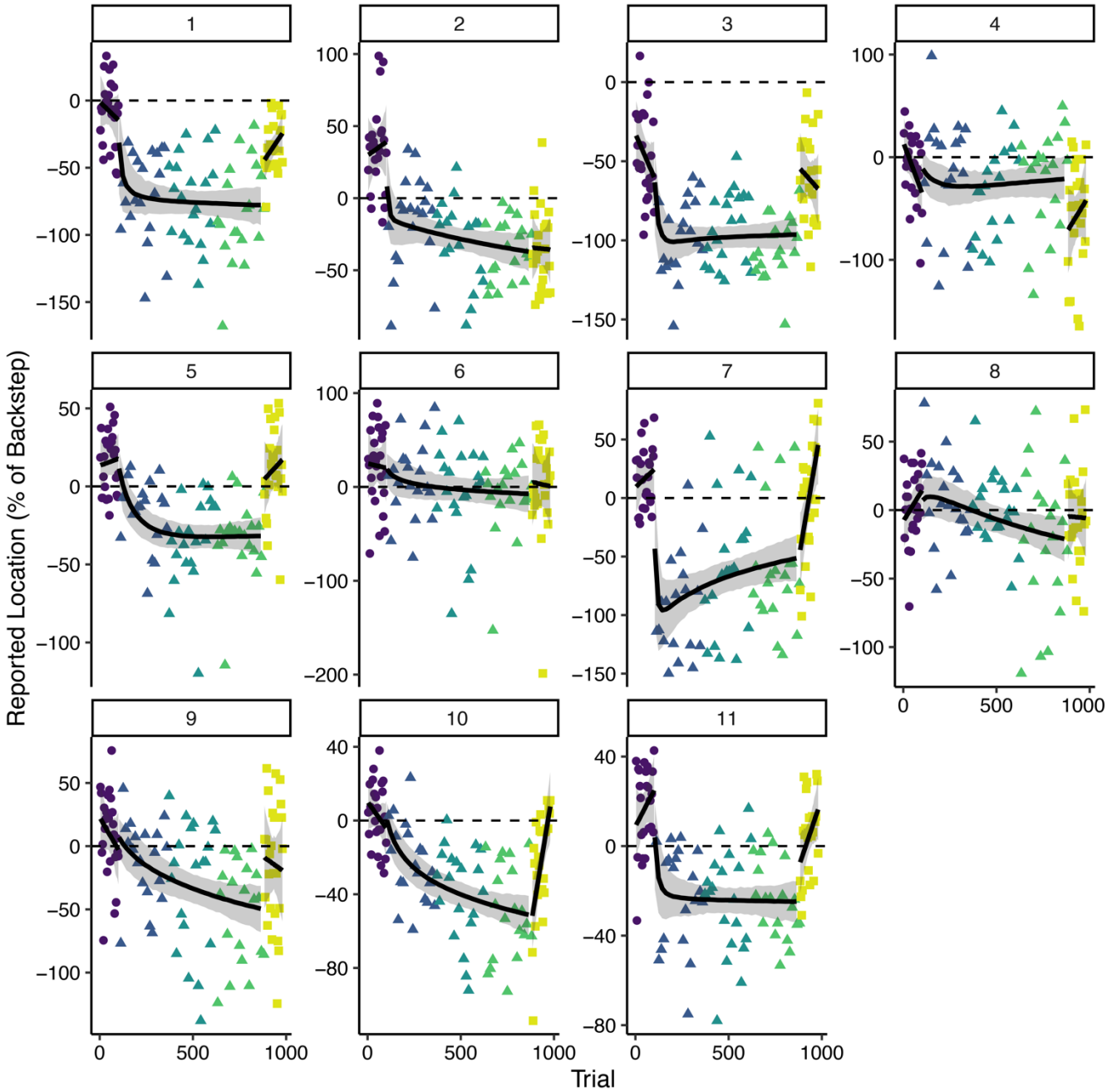

Supplementary Figure 6. Experiment 4 individual participant working memory recall timecourses. Individual data points represent trial recall location (N=11) as a percentage of the backstep size (3°) on Att-error trials for each WM-fixed trial. The target stimulus appeared at the same location in all data points shown (i.e. 0%). The *x*-axis represents the absolute trial number across all trial types (Att-error, WM-random, and WM-fixed). Color denotes block number and shape represents the phase of the experiment (pre-adapt, adapt, and post-adapt). The black lines spanning the pre- and post-adapt phases represent the mean of a linear model posterior predictive distribution, while the black line spanning the adapt phase is the mean of an exponential decay model posterior predictive distribution. The shaded area denotes the 95% credible interval of the expected value distribution for each model.

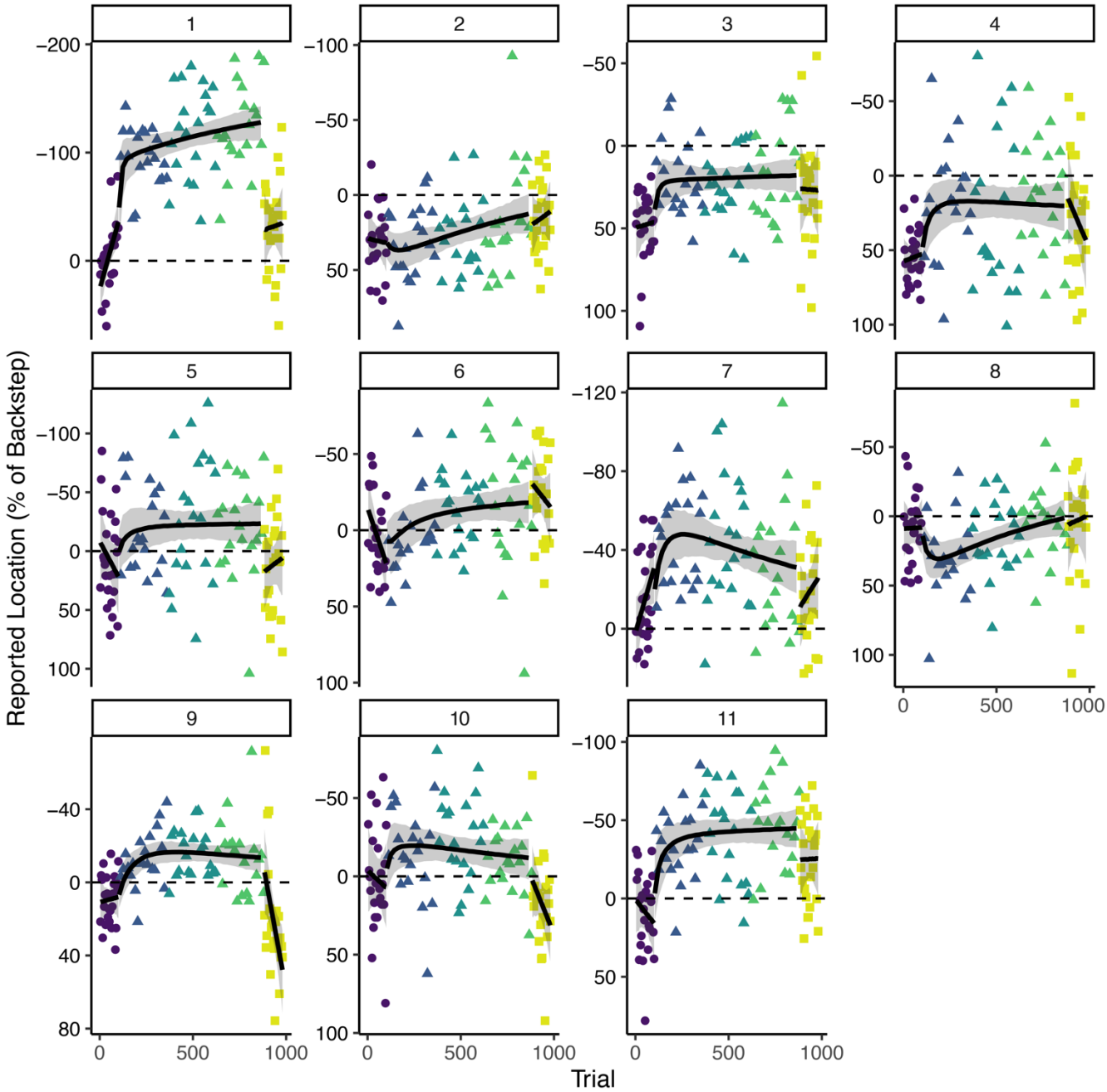

Supplementary Figure 7. Experiment 5 individual participant working memory recall timecourses. Individual data points represent trial recall location (N=11) as a percentage of the backstep size (3°) on Att-error trials for each WM-fixed trial. The target stimulus appeared at the same location in all data points shown (i.e. 0%). The *x*-axis represents the absolute trial number across all trial types (Att-error, WM-random, and WM-fixed). Color denotes block number and shape represents the phase of the experiment (pre-adapt, adapt, and post-adapt). The black lines spanning the pre- and post-adapt phases represent the mean of a linear model posterior predictive distribution, while the black line spanning the adapt phase is the mean of an exponential decay model posterior predictive distribution. The shaded area denotes the 95% credible interval of the expected value distribution for each model.